10^{th} International Conference on Fracture Mechanics of Concrete and Concrete Structures
FraMCoS-X
G. Pijaudier-Cabot, P. Grassl and C. La Borderie (Eds)
https://doi.org/10.21012/FC10.233192

MEASUREMENT OF FRACTURE ENERGY OF A HIGH PERFORMANCE CONCRETE IN DYNAMIC TENSION AND HIGH STRAIN RATES

BRATISLAV LUKIĆ[†], DOMINIQUE SALETTI[†*] AND PASCAL FORQUIN[†]

[†]Univ. Grenoble Alpes, CNRS, Grenoble INP*, 3SR, F-38000 Grenoble, France
*Institute of Engineering Univ. Grenoble Alpes
e-mail: dominique.saletti@3sr-grenoble.fr

Key words: High strain rate, Fracture energy, Concrete, The virtual fields method, Field measurements, Ultra high speed photography, The grid method

Abstract. This paper presents the experimental results of the dynamic fracture energy of HPC measured via the photomechanical spalling test. Full field measurements are performed and the stress - fracture opening displacement curves are obtained for each visualized fracture zone from which the specific fracture energy can be calculated. First results obtained from several spalling tests were found to be lower than what is reported in the literature.

1 INTRODUCTION

Concrete structures can get exposed to severe dynamic loadings such as blasts or impact over their service lifetime [1, 2]. These devastating scenarios need to be well taken into account in the structural design stage as well as in the choice of the optimal material composition. Advanced numerical modelling methods can be used to provide insight into the complexity of stress states that evolve in the material under such loading conditions. However, these material models need to be calibrated using a set of reliable experimental data obtained at corresponding range of strain rates. The specific fracture energy is one of the key parameters to be determined, since it plays an important role in calibrating non-linear constitutive models that are often used in the representation of damage or material softening response [3]. Nevertheless, this mechanical quantity is not easy to measure at high strain rates. The main difficulties arise from the intrinsic characteristics of concrete material, such as low tensile failure stress and small deformation capacity. Due to these reasons, the results currently present in the literature are scarce [4].

The spalling test technique which applies indirect tension in the tested material was formely used in a few works in order to obtain the information on the specific fracture energy [5–7]. However, due to mentioned experimental challenges, these methods had to rely on certain assumptions in the stage of data processing such as linear elastic material behaviour outside of fracture zone. Furthermore, the well documented phenomena of multiple crack formation with increasing strain rate influenced the use of notched samples which in turn can locally alter the stress state in the material [8,9], questioning the values of reported results.

Recently a method has been proposed to directly measure the specific fracture energy based on a photomechanical configuration of the spalling test [10]. An ultra high speed camera with an inter frame time down to 1 μs is used to obtain full field measurements on the sample surface during the test and the virtual fields method processing is used to relate the measured kinematics to the evolution of axial stress in the sample [11]. Thanks to this approach,

there is no necessity of assuming an *a priori* material behaviour to process the data and all the necessary information is obtained from the acquired images. Furthermore, thanks to having access to fields of displacement measurements the local fracturing content can be obtain for each visualized fracture. In that way there is no necessity of introducing a notch in the sample and the specific fracture energy can be measured for each observable crack.

In this work, this method is applied to testing high strength concrete (HPC). First the tested material is introduced as well as the experimental methodology. Next the data processing. Finally, obtained results are presented and compared to some previous ones obtained on ordinary concrete as well as those from the literature.

2 MATERIALS AND METHODS

2.1 Tested material

The concrete used in this work is a type of high strength concrete which is characterized by a strong cement matrix and a lower capillary porosity in comparisson to ordinary concrete [12]. The reduced porosity is achieved by adding silica fumes to the mix and subsequently decreasing the water-cement ratio to 0.3. Consequently the expected uniaxial compressive strength after 28 days is 80 MPa. The quantity of granulometric constituents was adjusted to achieve an adequate workability and the maximum aggregate size of 8 mm. This composition of the HPC used in this work and the mix proportions are given in Table 1.

Table 1: Composition of the HPC mixture used in this work.

Constituent	**[kg/m^3]**
Aggregates (D 0.5/8)	1008
Sand	795.4
Cement CEM 52.5	420
Superplasticizer	4.7
Silica fumes	46.7
Water	140

2.2 The photomechanical spalling test

The photomechanical spalling tests were performed in the Laboratory 3SR. The setup is based on a classical spalling experiment [13], which uses only the input Hopkinson bar (45 mm diameter and 1200 mm length) in order to exert tensile loading onto a cylindrical concrete sample (45 mm diameter and 140 mm length). The initial compressive pulse is generated with a cylindrical projectile (45 mm diameter and 50 mm length) that impacts the bar on one end and is transferred to the sample on the other end. Thanks to the sample intentional non-balanced state the compressive pulse reflects from the sample free-end into a tensile load. This makes the spalling test an adequate indirect dynamic tensile test for geomaterials such as rocks and concrete since it directly exploits the asymmetric nature of such materials. Thanks to the optimised geometry of the projectile and the impact velocity (5-10 m/s) the loading rate in the sample can be controlled. The photomechanical aspect of the tests reflects in the use of ultra-high speed imaging to measure the displacement fields on the sample surface throughout the whole test duration (around 80 μs). Owing to such short time duration, simulated experiments indicated that an adequate temporal discretisation which allows a reliable identification of an elastic response is 1 Mfps and above [14]. For this reason, the Shimadzu HPV-X2 camera was used to film a grid deposited on the sample surface. The acquisition system provides 128 images of 400x250 px count at 1 Mfps with exposure down to 200 ns. Some recent benchmark comparison showed that it provides a more stable acqusition sequence compared to some other imaging systems available [15]. A bi-directional grid of 1 mm pitch was deposited on the sample surface and was sampled with 5 px/mm, allowing the use of the grid method [16] in order to obtain 128 full field displacement maps on the observed surface of about 70x25 mm from the sample free-end. An example of the last recorded frame from one test is shown in Figure 1 and the corresponding displacement map

from one recording of the spalling test is presented in Figure 2.

Figure 1: Last recorded frame of a spalling test on HPC concrete with 1 Mfps acquisition speed. (Free-end on the left hand side)

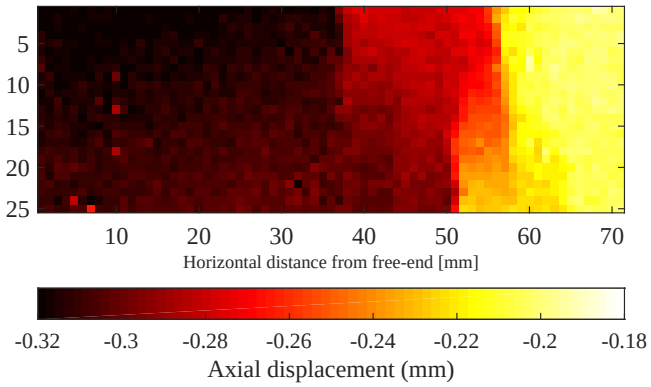

Figure 2: Axial displacement map corresponding to the image in Figure 1.

2.3 The virtual fields method processing

The virtual fields method is an identification technique which requires full-field measurments in the region of interest [17]. The identification procedure relies on rewriting the global equilibrium equation of a test case using the well-known principle of virtual work expressed with specific *a priori* chosen set of virtual fields. In recent years this procedure found a practical application in the dynamic testing of materials since it allows to exploit the inertial component of a dynamic test into its advantage. In the spalling test, the procedure provides a direct route towards measuring the evolution of average axial stress along the sample [11]. Introducing a rigid body virtual field into the weak form of the dynamic equilibrium equation, it is possible to reconstruct the average axial stress in any visualized cross-section by averaging the longitudinal acceleration over the area between the considered cross-section and the free-end. The resulting relation between the axial stress and the longitudinal acceleration is then expressed as:

$$\overline{\sigma(x,t)} = -\rho b(x)\overline{a_x(x,t)} \tag{1}$$

where $\overline{\sigma(x,t)}$ is the average axial stress in the cross-section at the observed position x from the sample free-end, $b(x)$ is the longitudinal distance from the free-end to the position x, $\overline{a_x(x,t)}$ is the average longitudinal acceleration on the area from the free-end to position x and ρ is material density.

3 RESULTS

3.1 Visualisation of fracture opening

Thanks to the large quantity of measured data contained in time resolved full-field displacement maps, the local behaviour around each observable displacement discontinuity can be analysed in a quantitative manner. The time evolution of these discontinuities is interesting to be analysed since they can present potential fracture zones which are created during the test. In order to verify their actual state, first a virtual differential-displacement gauge can be introduced around each such zone within 2 mm distance from each side. This virtual tool acts as a local differential extensometer. Then, thanks to the local measurement of stress (encoded in the acceleration fields) and the local measurement of strain (encoded through spatial gradient of displacement fields) the elastic component of the differential displacement can be substracted from the virtual differential gauge, providing what is refered to in [10] the fracture opening displacement (FOD). An example of such measurement for the two potential fracture zones for the test case presented in Figure 2, is given in Figure 3. Analysing the presented plot, it is interesting to note that the fracture at 38

mm appears to be initiated before the fracture at 56 mm. However, it reaches a plateau and remains still while the fracture at 56 mm becomes the dominant fracture that continues to propagate. Indeed, in this case, only the macro-crack at 56 mm was observed by naked eye in the post-mortem overview of the sample.

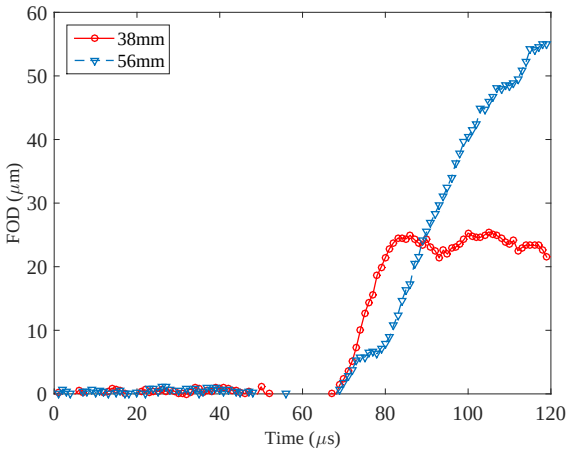

Figure 3: Time evolution of the fracture opening displacement (FOD) for two characteristic locations in Figure 2.

3.2 Reconstruction of the S-FOD curves

Since it is demonstrated that both the average axial stress and the average local fracture opening displacement can be directly extracted from the same time resolved displacement fields around one fracture zone, the two measurements can be combined to form a Stress-Fracture opening displacement curve (S-FOD). The area below this curve directly provides the value of the specific fracture energy with no need for an additional measurement of the fractured surface. Furthermore such a curve can be traced for any visualized fracture zone, providing multiple values of specific fracture energy from only one spalling test. One example of such curve from one spalling test on HPC that presented a single open fracture is presented in Figure 4.

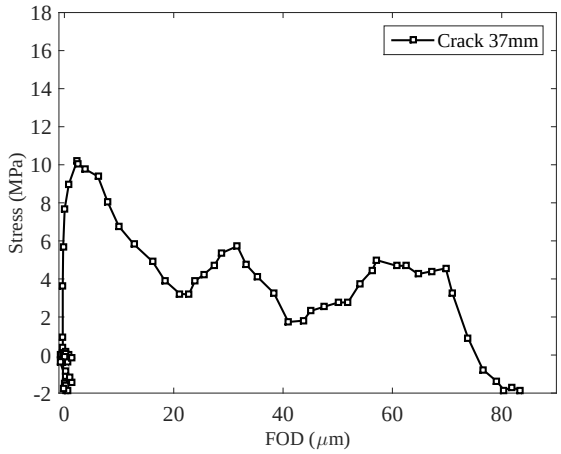

Figure 4: Stress-Fracture opening displacement curve obtained via photomechanical analysis of a spalling test on HPC.

3.3 Results and comparison

In total 6 spalling tests were performed on HPC samples and the above described methodology was performed in order to obtain specific fracture energy information. The data is presented in Figure 5 with respect to fracture opening velocity. When compared to the data from the literature [18], the results from this work are notable lower. On the other hand, when results on HPC are compared to the values obtained on ordinary concrete using the same methodology, no notable difference can be observed.

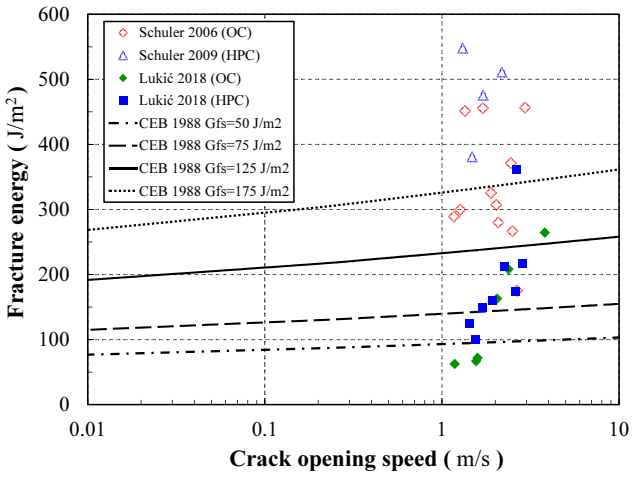

Figure 5: Results on the specific fracture energy [19].

4 CONCLUSIONS AND PERSPECTIVES

In this work a photomechanical spalling method is applied to extract the values of specific fracture energy from spalling tests performed on a type of high strength concrete. The methodology allows obtaining one value of specific fracture energy per each visualized fracture with an ultra high speed camera, exploiting the local data content from the time resolved full-field displacement maps. Some of the first results are found to be notable lower than those reported in the literature.

Acknowledgements

The authors would like to express their gratitude to LMT Cachan for supplying the ultra-high-speed acquisition system.

REFERENCES

[1] Daudeville, L., and Malecot, Y. 2011. Concrete structures under impact. *Journal of Environmental and Civil Engineering* **15**:101–140.

[2] Li, Q.M., Reid, S.R., Wen, H.M., Telford, A.R. 2005. Local impact effects of hard missiles on concrete target. *International Journal of Impact Engineering* **32**:224–284.

[3] Mazars, J. 1986. A description of micro- and macroscale damage of concrete structures. *Engineering Fracture Mechanics* **25**:729–737.

[4] Weerheijm, J., 2010. The dynamic fracture energy of concrete: Review of test methods and data comparison. *Proceedings of FraMCoS-7*.

[5] Schuler, H., Mayrhofer, C., Thoma, K. 2006. Spall experiments for the measurement of the tensile strength and fracture energy of concrete at high strain rates. *International Journal of Impact Engineering* **32**:1635–1650.

[6] Weerheijm, J., Van Doormaal, J.C.A.M. 2007. Tensile failure of concrete at high loading rates: New test data on strength and fracture energy from instrumented spalling tests. *International Journal of Impact Engineering* **34**:609–629.

[7] Rey-de-Pedraza, V., Gálvez, F., Cendón Franco, D. 2018. Measurement of fracture energy of concrete at high strain rates. *EPJ Web of Conferences* **183**:02065.

[8] Schuler, H. 2007. Evaluation of an experimental method via numerical simulations. *Proceedings of FraMCoS-6*.

[9] Van Doormaal, J.C.A.M, Weerheijm, J., Sluys, L. 1994. Evaluation of an experimental method via numerical simulations. *Journal de Physique IV* **4**:501-506.

[10] Lukić, B., Saletti, D., Forquin, P. 2018. On the Processing of Spalling Experiments. Part II: Identification of Concrete Fracture Energy in Dynamic Tension. *Journal of Dynamic Behavior of Materials* **4**:56-73.

[11] Pierron, F., Forquin, P. 2012. Ultra-High-Speed Full-Field Deformation Measurements on Concrete Spalling Specimens and Stiffness Identification with the Virtual Fields Method. *Strain* **48**:388-405.

[12] Malecot, Y., Zingg, L., Briffaut, M., Baroth, J. 2019. Influence of free water on concrete triaxial behavior: The effect of porosity. *Cement and Concrete Research* **120**:207-216.

[13] Erzar, B., Forquin, P. 2010. An Experimental Method to Determine the Tensile Strength of Concrete at High Rates of Strain. *Experimental Mechanics* **50**:941-955.

[14] Lukić, B., Saletti, D., Forquin, P. 2017. Use of simulated experiments for material characterization of brittle materials subjected to high strain rate dynamic tension. *Philosophical Transactions of the Royal Society A* **375**:20160168.

[15] Forquin, P., Lukić, B., Saletti, D., Sallier, L., Pierron, F. 2019. A benchmark testing technique to characterize the stress-strain relationship in materials based on the spalling test and a photomechanical method. *Measurement Science and Technology*.

[16] Grédiac, M., Sur, F., Blaysat, B. 2016. The Grid Method for In-plane Displacement and Strain Measurement: A Review and Analysis. *Strain* **52**:205-243.

[17] Pierron, F., and Grédiac, M. 2012. *The Virtual Fields Method*, Springer-Verlag, New York (1st ed., 2012, 518 pp.).

[18] Schuler, H., Hansson, H. 2006. Fracture behaviour of High Performance Concrete (HPC) investigated with a Hopkinson-Bar. *Journal de Physique IV* **134**:1145-1151.

[19] Lukić, B. 2018. Development of a full-field measuring technique for the characterisation of the dynamic tensile behaviour of concrete. *Université Grenoble Alpes*, Doctoral thesis.